J. Phys. Ther. Sci. 35: 156–162, 2023

The Journal of Physical Therapy Science

Technical Note

Applicability of automated tractography during acute care stroke rehabilitation

Midori Mochizuki, MD[1)*], Yuki Uchiyama, MD, PhD[2)], Kazuhisa Domen, MD, PhD[2)], Tetsuo Koyama, MD, PhD[1, 2)]

[1)] *Department of Rehabilitation Medicine, Nishinomiya Kyoritsu Neurosurgical Hospital: 11-1 Imazu-Yamanaka-cho, Nishinomiya, Hyogo 663-8211, Japan*
[2)] *Department of Rehabilitation Medicine, Hyogo Medical University, Japan*

Abstract. [Purpose] To assess the clinical applicability of a novel automated tractography tool named XTRACT during acute stroke rehabilitation. [Participants and Methods] Three patients with left hemisphere stroke were sampled. Diffusion tensor images were acquired on the second week, and automated tractography was then applied. Tractography images and fractional anisotropy (FA) values in the corticospinal tract (CST) and arcuate fasciculus (AF) were assessed in relation to hemiparesis and aphasia. [Results] Patient 1 was nearly asymptomatic; FA in the left CST was 0.610 and that in the AF was 0.509. Patient 2 had severe hemiparesis and mild motor aphasia. Tractography images of the CST and AF were blurred; FA in the left CST was 0.295 and that in the AF was 0.304. Patient 3 showed no hemiparesis or aphasia at initial assessment. Tractography image of the CST was intact but that of the AF was less clear; FA in the left CST was 0.586 and that in the AF was 0.338. Considering the less clear images of the AF and lower FA value in Patients 2 and 3, further examinations for aphasia were performed, which revealed agraphia. [Conclusion] Visualization and quantification of neural fibers using automated tractography promoted planning acute care rehabilitative treatment in patients with stroke.
Key words: Automatic, Neuroimaging, Visualization

(This article was submitted Oct. 24, 2022, and was accepted Nov. 22, 2022)

INTRODUCTION

Neuroimaging is essential in the treatment of stroke patients. Imaging techniques such as computed tomography (CT) and magnetic resonance imaging (MRI) are used to schedule appropriate rehabilitative treatments[1)]. Among the various neuroimaging techniques available, diffusion tensor imaging (DTI) is the only tool that enables *in vivo* assessment of degeneration of neural fibers in relation to clinical symptoms[2, 3)]. Previous studies have investigated the relationship between neural degeneration of the corticospinal tract (CST) and motor outcomes[4, 5)], as well as that between neural damage to association fibers and cognitive decline[6, 7)]. However, most of these studies employed the fractional anisotropy (FA) value, which is considered to indicate Wallerian degeneration due to stroke[8)].

Tractography is an analytical DTI methodology that enables visualization as well as calculation of FA values and tract volumes but requires a start point (seed) and end point (target), which are usually defined manually[9)]. It is also time-consuming, subjective, and less accurate than other analytical DTI methodologies in terms of reproducibility. An automated procedure known as XTRACT has been developed to compensate for these disadvantages[10)]. This method uses predetermined parameter settings required for tractography analyses, including seed, target, exclusion masks, and number of samples. XTRACT routinely extracts 42 tracts, including the CST, arcuate fasciculus (AF), and uncinate fasciculus[10)]. The simplicity of this

*Corresponding author. Midori Mochizuki (E-mail: midori.tanaka625@gmail.com)

procedure may facilitate its application in the clinical setting. In this report, we describe the clinical value of this automated tractography tool when designing rehabilitative treatment in the acute phase after stroke at a community-based hospital in Japan.

PARTICIPANTS AND METHODS

This study included patients with typical hemorrhagic or ischemic stroke who were admitted to Nishinomiya Kyoritsu Neurosurgical Hospital in April or May 2022. All patients were transferred to our hospital soon after onset and underwent brain CT and MRI. CT scans and diffusion-weighted imaging (DWI) were reviewed by our medical staff. Image acquisition protocols for CT and DWI are described in our previous reports[11, 12]. Given that the purpose of this study was to assess the clinical value of automated tractography in stroke rehabilitation, we selected three typical cases with left hemisphere lesions: one was asymptomatic, one had hemiparesis with aphasia, and one had aphasia without hemiparesis. None of the patients had a known neurological disorder before onset of stroke.

The protocol for treatment of stroke in these patients followed the methods stated in the Japanese Guidelines for the Management of Stroke 2021[13]. The patients received conservative treatments such as medication (e.g., antihypertensive agents for hemorrhagic stroke, and anticoagulant or antiplatelet agents for ischemic stroke). During hospitalization, they also underwent rehabilitation, consisting of physical, occupational, and speech therapy for a combined daily total of up to 180 min. The study protocol was approved by our institutional ethics committee on June 20, 2022. The patients (or relatives when necessary) provided written informed consent for inclusion in this report.

Typical clinical symptoms of left hemisphere stroke are right hemiparesis and aphasia. The severity of these two symptoms was evaluated using the Brunnstrom recovery stage (BRS)[14, 15] and Standard Language Test of Aphasia (SLTA)[16, 17]. The BRS evaluates the function of the proximal (shoulder, elbow, forearm) and distal (hand) upper extremity and lower extremity on a 6-point scale (I, severe; VI, normal). The SLTA is the most widely used comprehensive test battery in Japan and consists of 26 subtests that evaluate hearing, speaking, reading, writing, and calculation ability.

MRI was usually performed in the second week after admission to our acute care service using a 3.0-Tesla scanner (MAGNETOM Trio; Siemens AG, Erlangen, Germany) with a 32-channel head coil. The DTI data were obtained using a single-shot echo-planar imaging sequence (anterior-to-posterior direction) and consisted of 30 images with non-collinear diffusion gradients (b=1500 s/mm^2) and one non-DWI scan (b=0 s/mm^2). Eighty contiguous axial slices were obtained for each patient. The field of view was 256 mm × 256 mm, the acquisition matrix was 128 × 128, and the slice thickness was 2 mm. The echo time was 96 ms, the repetition time was 10,900 ms, and the flip angle was 90 degrees. For the purpose of correcting eddy-current and echo-planar imaging-induced distortions, two non-DWI scans in the anterior-to-posterior direction and two additional non-DWI scans in the posterior-to-anterior direction were then acquired. To obtain the anatomical details of the patients' brains, T1-weighted images were also acquired using a three-dimensional fast gradient imaging sequence. A total of 176 contiguous sagittal slices were obtained for each patient. The field of view was 256 mm × 256 mm, the acquisition matrix was 256 × 256, and the slice thickness was 1 mm. The echo time was 1,900 ms, the repetition time was 2.52 ms, and the flip angle was 10 degrees.

MRtrix[18] and the FMRIB Software Library (FSL)[19] were used for image processing. First, all DTI scans were denoised. The Gibbs ringing artifact was then removed using the "dwidenoise" and "mrdegibbs" commands implemented in MRtrix[20, 21]. Next, eddy-current and echo-planar imaging-induced distortions were corrected using the "topup" and "eddy" commands implemented in FSL[22, 23]. Bias-field corrections were performed using the "dwibiascorrect" command in MRtrix with the "ants" option[24]. Thereafter, brain masks for data analyses were generated from the bias-field-corrected images using the "dwi2mask" command in MRtrix[25].

After the above-mentioned preprocessing stages, a diffusion tensor at each voxel was modeled for each patient using the DTIFIT tool in FSL. As preparation for the tractography procedures, four-dimensional DTI data were taken into the BEDPOSTX tool in FSL to calculate the Bayesian estimate of diffusion parameters[26, 27]. Finally, to perform tractography, the output of the previous step was fed into the XTRACT tool[10] in FSL, which automatically extracts 42 tracts for each patient. The normalized tract density for each tract was stored in the Montreal Neuroimaging Institute (MNI) standard space. Default settings were used for these procedures in view of the aim of the study, which was to assess the clinical value of the XTRACT tool in stroke rehabilitation.

From the obtained tractography images, parameter estimates, including FA values and tract volumes, were abstracted by the "xtract_stats" command in FSL. In this step, we set the threshold at 0.01 in reference to the FA values reported in our previous DTI studies[6, 7]. All procedures used for the tractography calculations were performed in the native space for each patient. However, to facilitate visualization, tract images were co-registered in the MNI standard brain.

The XTRACT tool in FSL tracks 42 neural tracts within the brain, including projection, association, and commissural fibers. However, for clarity, we limited our investigations to the CST and AF for two reasons: (1) our previous DTI studies, which focused on stroke patients with supratentorial lesions, indicated that the most severely damaged neural tracts were the CST and AF, and (2) the CST is correlated with motor-related symptoms such as hemiparesis, and the AF is associated with cognition-related symptoms such as aphasia[6, 7, 28].

RESULTS

Table 1 summarizes the patients' characteristics and Fig. 1 shows the brain images obtained on admission. Cases 1 and 3 had ischemic stroke and Case 2 had hemorrhagic stroke. Case 1 showed high-intensity areas in the postcentral gyrus and was asymptomatic in terms of motor and cognitive function. Case 2 showed intracerebral hemorrhage in the putamen and had severe hemiparesis and aphasia. Case 3 showed high-intensity areas in the temporal lobe and had aphasia without hemiparesis. The following sections provide a detailed description of each of the three cases and the findings on automated tractography images.

For Case 1, the patient was an 80-year-old female who visited our hospital complaining of sudden onset of numbness in her right forearm after previously being independent in activities of daily living. She was examined by MRI. DWI scans showed high-intensity areas in the left postcentral gyrus (Fig. 1). She was diagnosed with atherosclerotic ischemic stroke and was treated conservatively. Her motor functions were intact and her gait, posture, and hand dexterity were normal. She showed no signs of aphasia; her speech was fluent and she fully understood and signed the consent forms. Tractography images of the CST and AF in both hemispheres were clearly traced (Fig. 2); the FA values were correspondingly intact for the CST and AF (Table 1). The numbness in the patient's right forearm disappeared and she was discharged home on day 9.

For Case 2, the patient was a 58-year-old male who was transferred to our acute care service after sudden onset of right hemiparesis and dysarthria while at work. CT images acquired on admission showed high-density areas in the left putamen (Fig. 1). He was treated with antihypertensive medication. He had severe right hemiparesis indexed by BRS as I-I-I. He also had severe sensory loss in the right upper and lower extremities. The patient was predicted to have severe aphasia in view of the size of the lesions seen on the CT images[7]. However, during the first medical round, a physiatrist (M.M.) noticed that his listening comprehension was well preserved and that he had only slight motor aphasia. A detailed evaluation using the SLTA revealed a low score for word repetition and writing *kanji* (Chinese characters regularly used in daily Japanese writing).

Table 1. Patient demographics and clinical characteristics

Case no. (age, gender)		1 (80, F)	2 (58, M)	3 (51, M)
Stroke type		Ischemic	Hemorrhagic	Ischemic
Lesion		Left postcentral gyrus	Left putamen	Left temporal lobe
Hemiparesis (BRS)		None	I - I - I	None
Aphasia		None	Word repetition disorder, agraphia	Agraphia
Fractional Anisotropy (R/L)	CST	0.630/0.610	0.595/0.295	0.600/0.586
	AF	0.520/0.509	0.452/0.304	0.538/0.338
Tract volume (mL) (R/L)	CST	2.056/2.352	2.552/5.080	2.832/2.216
	AF	1.416/1.912	1.696/2.472	1.760/1.696
Waytotal (R/L)	CST	154163/74181	211478/174	152006/90157
	AF	1428038/1708963	2372769/439609	1609581/1375835

AF: arcuate fasciculus; BRS: Brunnstrom recovery stage (shoulder/elbow/forearm-hand-lower extremity, 6-point scale [I, severe; VI, normal]); CST: corticospinal tract; F: female; L: left; M: male; R: right.

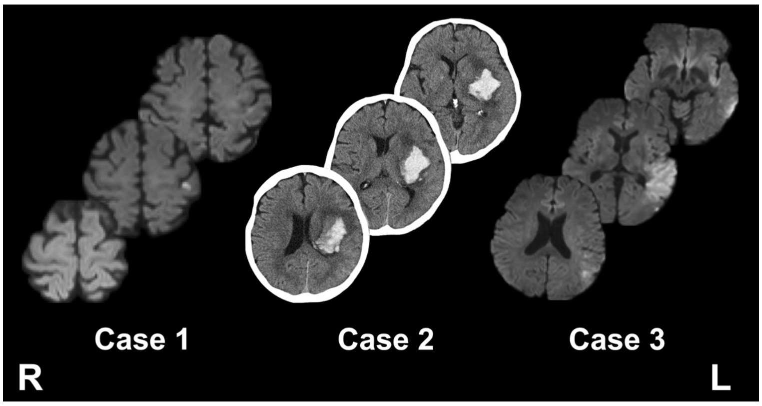

Fig. 1. Diffusion-weighted magnetic resonance images (Cases 1 and 3) and computed tomography images (Case 2) for the three patients included in this report. L: left; R: right.

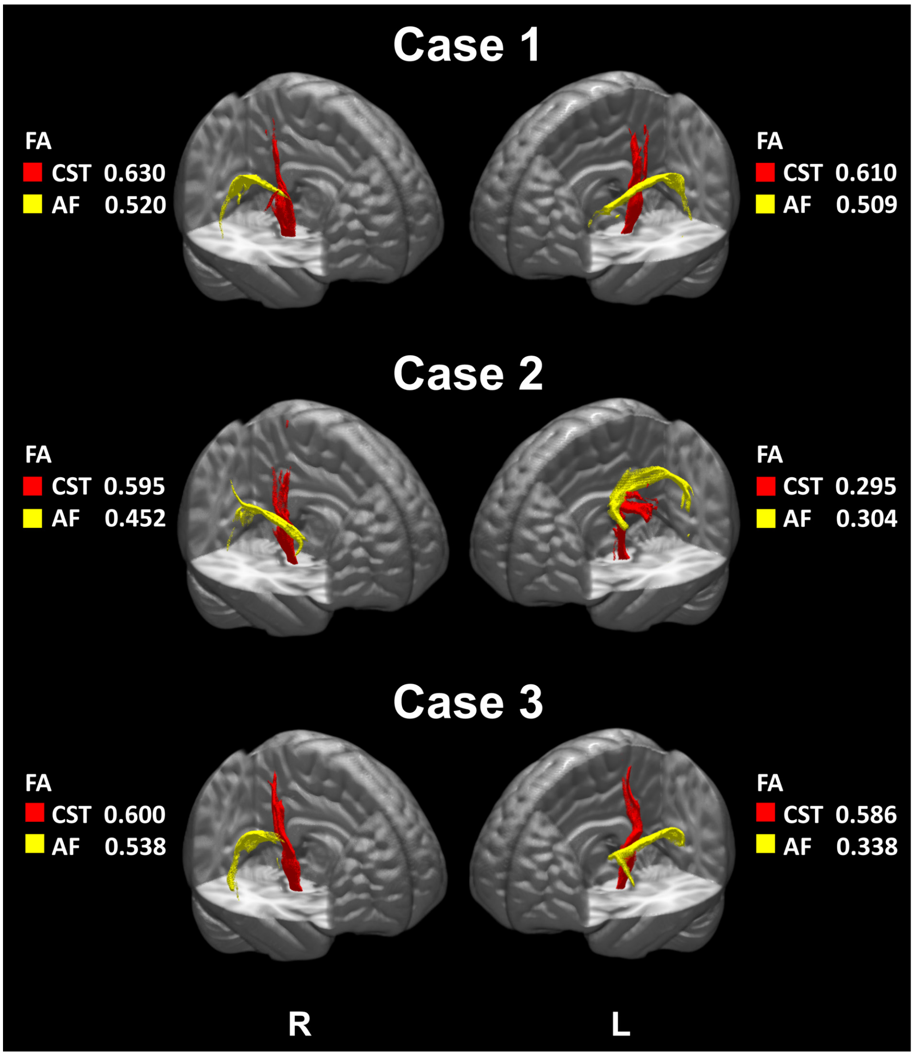

Fig. 2. Three-dimensional images obtained by automated tractography. The red areas show the corticospinal tract and the yellow areas show the arcuate fasciculus. Diffusion tensor imaging-fractional anisotropy values are shown for both tracts. AF: arcuate fasciculus; CST: corticospinal tract; FA: fractional anisotropy; L: left; R: right.

Tractography images of the CST in the lesioned left hemisphere were disrupted in the corona radiata area and those of the AF were blurred in the middle portion (Fig. 2). These findings were consistent with the FA values obtained (CST, 0.295; AF 0.304) (Table 1). After completion of treatment in the acute phase, he had severe hemiparesis with BRS II-I-III and aphasia. He was transferred to our affiliated rehabilitation hospital on day 29 to continue rehabilitative treatments.

For Case 3, the patient was a 51-year-old male who was transferred to our acute care service after sudden onset of right hemiparesis and dysarthria. DWI scans obtained on admission showed high-intensity areas in the left insula and magnetic resonance angiography revealed occlusion of the left anterior temporal artery. He was diagnosed with thromboembolic ischemic stroke and treated with intravenous tissue plasminogen activator and thrombectomy followed by anticoagulant medication. The DWI scans acquired on day 2 showed high-intensity areas in the left temporal lobe (Fig. 1). No hemiparesis was noted during the initial assessment for rehabilitative treatment, and his gait, posture, and hand dexterity were intact. He was able to comprehend and speak fluently without dysarthria. However, on day 9, he noticed difficulty in writing *kanji*. A detailed examination was performed using the SLTA, which showed low scores for writing *kanji* and calculation. The tractography images of the CST in the left hemisphere were comparable with those obtained for Case 1, which had been asymptomatic; however, the tractography image for the AF was less clear in the posterior area (Fig. 2). These findings were consistent with the FA values obtained (CST, 0.586; AF, 0.338) (Table 1). In order to return to work as the owner of a painting business, he needed to regain his ability to take notes (e.g., write appointment reminders) and do calculations (e.g., quotations). He was transferred to our affiliated rehabilitation hospital on day 17 for the further rehabilitative treatments needed for return to work.

DISCUSSION

In this report, we describe our clinical experience of the value of automated tractography when planning appropriate rehabilitative treatments for patients receiving acute care after stroke. Three representative patients with left hemisphere lesions were investigated in detail. Case 2 had a putaminal hemorrhage. As expected from the CT images obtained on admission, he developed severe hemiparesis. The tractography images for this patient indicated disruption and a decreased FA for the CST and corresponded to the conventional CT images. Meanwhile, Cases 2 and 3 developed aphasia. Initially, they were able to communicate verbally with our medical staff members. In both cases, the aphasia was less severe than expected from the conventional neuroimages obtained on admission. However, further investigation for aphasia revealed agraphia when writing *kanji*. The findings on the automated tractography images of the AF were consistent with these symptoms and facilitated implementation of a rehabilitation program focused on recovery from aphasia.

The automated tractography images also enabled quantitative assessment of FA values, which are associated with the severity of symptoms. In previous studies on tract-based spatial statistics, we investigated the relationship between FA values and the severity of motor and cognitive outcomes in stroke patients[6, 7] and found that a lower value in the CST heralded a more severe motor outcome and that a lower value in the AF was associated with a poorer cognitive outcome. For the patient in Case 2, who developed severe hemiparesis, the FA value for the CST in the lesioned hemisphere was 0.295. According to our preliminary findings in 20 stroke patients similar to those described in this report, the median FA value for the CST in the non-lesioned hemisphere was 0.572 (interquartile range 0.552–0.633). Moreover, the FA value for the AF in the lesioned hemisphere was 0.304 for Case 2 and 0.338 for Case 3 presented here, whereas the median FA value in our preliminary analysis was 0.465 (interquartile range 0.447–0.486). However, the relationship between the FA value assessed by automated tractography and symptom severity has yet to be investigated.

Automated tractography allows visualization of the neural tracts. The tractography images of the CST and AF were clearly traced in both hemispheres for Case 1 but were blurred in the lesioned left hemisphere for Case 2 (Fig. 2). Visualization of the neural tracts on automated tractography images facilitated comprehension of the findings of DTI. The findings on DTI need to be presented in a comprehensive manner in view of the multidisciplinary nature of rehabilitation services[13]. At our acute care facility, three-dimensional tractography images and FA values (as outlined in Fig. 2) are shared during weekly interdisciplinary meetings. Indeed, our experience has indicated that automated tractography is clinically useful in stroke rehabilitation.

Most of the research on tractography has employed density distributions normalized by the “waytotal”[29, 30], which represents the total amount of streamline numbers that were not rejected by the exclusion masks. The automated tractography technique applied in this study, namely, XTRACT, uses the same normalization procedure. However, this procedure may require some attention. In our preliminary analysis of patients with severe stroke, there were some cases in which the waytotal value was extremely low. In our Case 2, the FA value for the left CST was lower than that for the right, reflecting the severe right hemiparesis. However, the tract volume was higher in the lesioned left hemisphere. In cases with extremely low waytotal values, the tract volume may be large. Therefore, the values obtained in such cases require careful interpretation.

The purpose of this research was to describe the clinical applicability of automated tractography at a community-based acute care hospital. Using a regular Macintosh desktop computer (Mac Studio with Apple M1 Max chip; Apple Inc., Cupertino, CA, USA), it takes us approximately 20 h to complete the whole analytical procedure for an individual patient. Nevertheless, we still consider this technique to be useful in daily clinical practice. Importantly, we use an analytical pipeline written in UNIX shell script, which is practical in the setting of stroke rehabilitation because the neural tracts can be assessed automatically overnight without any manual input. Recent technological advances have allowed use of graphics processing units (GPUs) to accelerate DTI analyses[31, 32]. However, due to technical difficulties, we could not use a GPU setting. Easier access to GPU settings in regular desktop computers (e.g., Macs and Windows) is required.

This study had several limitations. First, tractography evaluations, including FA values and tract volumes, depend heavily on parameter settings, such as thresholding. To date, there have been no consensus regarding which settings are optimal. Second, we focused solely on the AF as a neural tract responsible for aphasia. However, other neural tracts, including the inferior fronto-occipital fasciculus, middle longitudinal fasciculus, inferior longitudinal fasciculus, and uncinate fasciculus have been reported to be associated with aphasia[33–36]. These tracts are also indexed by XTRACT. However, in this study, we only sampled the AF relative to aphasia for clarity. Third, the relationships between parameter estimates (e.g., FA) from the automated tractography images and long-term outcomes (e.g., 3–6 months after stroke onset) remain unclear. In our previous DTI studies, which used analytical methodologies other than automated tractography, FA values were related to long-term outcomes such as hemiparesis and ability to perform activities of daily living[7, 37]. Knowledge about such relationships enables outcomes to be predicted during the acute phase, and studies are needed on this issue. Despite these limitations, our clinical experience has shown that automated tractography in stroke patients is useful during acute rehabilitation in the community-based hospital setting.

Funding

This work was supported in part by a Grant-in-Aid for Scientific Research (C) from the Japan Society for the Promotion of Science (JSPS KAKENHI Grant Number JP22K11356), and by a Grant-in-Aid for Scientific Research on Innovative Areas—Platforms for Advanced Technologies and Research Resources "Advanced Bioimaging Support" (JSPS KAKENHI Grant Number JP16H06280).

Conflict of interest

The authors declare that there are no conflicts of interest.

REFERENCES

1) Boyd LA, Hayward KS, Ward NS, et al.: Biomarkers of stroke recovery: consensus-based core recommendations from the Stroke Recovery and Rehabilitation Roundtable. Int J Stroke, 2017, 12: 480–493. [Medline] [CrossRef]
2) Yamada K, Sakai K, Akazawa K, et al.: MR tractography: a review of its clinical applications. Magn Reson Med Sci, 2009, 8: 165–174. [Medline] [CrossRef]
3) Kunimatsu A, Aoki S, Masutani Y, et al.: Three-dimensional white matter tractography by diffusion tensor imaging in ischaemic stroke involving the corticospinal tract. Neuroradiology, 2003, 45: 532–535. [Medline] [CrossRef]
4) Kim B, Winstein C: Can neurological biomarkers of brain impairment be used to predict poststroke motor recovery? A systematic review. Neurorehabil Neural Repair, 2017, 31: 3–24. [Medline] [CrossRef]
5) Koyama T, Uchiyama Y, Domen K: Outcome in stroke patients is associated with age and fractional anisotropy in the cerebral peduncles: a multivariate regression study. Prog Rehabil Med, 2020, 5: 20200006. [Medline]
6) Koyama T, Domen K: Diffusion tensor fractional anisotropy in the superior longitudinal fasciculus correlates with functional independence measure cognition scores in patients with cerebral infarction. J Stroke Cerebrovasc Dis, 2017, 26: 1704–1711. [Medline] [CrossRef]
7) Koyama T, Uchiyama Y, Domen K: Associations of diffusion-tensor fractional anisotropy and FIM outcome assessments after intracerebral hemorrhage. J Stroke Cerebrovasc Dis, 2018, 27: 2869–2876. [Medline] [CrossRef]
8) Yu C, Zhu C, Zhang Y, et al.: A longitudinal diffusion tensor imaging study on Wallerian degeneration of corticospinal tract after motor pathway stroke. Neuroimage, 2009, 47: 451–458. [Medline] [CrossRef]
9) Jones DK: Studying connections in the living human brain with diffusion MRI. Cortex, 2008, 44: 936–952. [Medline] [CrossRef]
10) Warrington S, Bryant KL, Khrapitchev AA, et al.: XTRACT—standardised protocols for automated tractography in the human and macaque brain. Neuroimage, 2020, 217: 116923. [Medline] [CrossRef]
11) Koyama T, Marumoto K, Miyake H, et al.: Relationship between diffusion tensor fractional anisotropy and long-term motor outcome in patients with hemiparesis after middle cerebral artery infarction. J Stroke Cerebrovasc Dis, 2014, 23: 2397–2404. [Medline] [CrossRef]
12) Uchiyama Y, Domen K, Koyama T: Outcome prediction of patients with intracerebral hemorrhage by measurement of lesion volume in the corticospinal tract on computed tomography. Prog Rehabil Med, 2021, 6: 20210050. [Medline]
13) Miyamoto S, Ogasawara K, Kuroda S, et al. Committee for Stroke Guideline 2021, the Japan Stroke Society: Japan Stroke Society Guideline 2021 for the treatment of stroke. Int J Stroke, 2022, 17: 1039–1049. [Medline] [CrossRef]
14) Safaz I, Yilmaz B, Yaşar E, et al.: Brunnstrom recovery stage and motricity index for the evaluation of upper extremity in stroke: analysis for correlation and responsiveness. Int J Rehabil Res, 2009, 32: 228–231. [Medline] [CrossRef]
15) Naghdi S, Ansari NN, Mansouri K, et al.: A neurophysiological and clinical study of Brunnstrom recovery stages in the upper limb following stroke. Brain Inj, 2010, 24: 1372–1378. [Medline] [CrossRef]
16) Mimura M, Kato M, Kato M, et al.: Prospective and retrospective studies of recovery in aphasia. Changes in cerebral blood flow and language functions. Brain, 1998, 121: 2083–2094. [Medline] [CrossRef]
17) Suzuki Y: Selection of neuropsychological tasks from a language test battery that optimally related to the function of each cortical area: toward making a cognitive cortical map. Neuroimage Clin, 2019, 22: 101799. [Medline] [CrossRef]
18) Tournier JD, Smith R, Raffelt D, et al.: MRtrix3: a fast, flexible and open software framework for medical image processing and visualisation. Neuroimage, 2019, 202: 116137. [Medline] [CrossRef]
19) Jenkinson M, Beckmann CF, Behrens TE, et al.: FSL. Neuroimage, 2012, 62: 782–790. [Medline] [CrossRef]
20) Veraart J, Fieremans E, Novikov DS: Diffusion MRI noise mapping using random matrix theory. Magn Reson Med, 2016, 76: 1582–1593. [Medline] [CrossRef]
21) Kellner E, Dhital B, Kiselev VG, et al.: Gibbs-ringing artifact removal based on local subvoxel-shifts. Magn Reson Med, 2016, 76: 1574–1581. [Medline] [CrossRef]
22) Andersson JL, Skare S, Ashburner J: How to correct susceptibility distortions in spin-echo echo-planar images: application to diffusion tensor imaging. Neuroimage, 2003, 20: 870–888. [Medline] [CrossRef]
23) Andersson JL, Sotiropoulos SN: An integrated approach to correction for off-resonance effects and subject movement in diffusion MR imaging. Neuroimage, 2016, 125: 1063–1078. [Medline] [CrossRef]
24) Tustison NJ, Avants BB, Cook PA, et al.: N4ITK: improved N3 bias correction. IEEE Trans Med Imaging, 2010, 29: 1310–1320. [Medline] [CrossRef]
25) Veraart J, Sijbers J, Sunaert S, et al.: Weighted linear least squares estimation of diffusion MRI parameters: strengths, limitations, and pitfalls. Neuroimage, 2013, 81: 335–346. [Medline] [CrossRef]
26) Behrens TE, Berg HJ, Jbabdi S, et al.: Probabilistic diffusion tractography with multiple fibre orientations: what can we gain? Neuroimage, 2007, 34: 144–155. [Medline] [CrossRef]
27) Jbabdi S, Sotiropoulos SN, Savio AM, et al.: Model-based analysis of multishell diffusion MR data for tractography: how to get over fitting problems. Magn

Reson Med, 2012, 68: 1846–1855. [Medline] [CrossRef]
28) Koyama T, Domen K: Reduced diffusion tensor fractional anisotropy in the left arcuate fasciculus of patients with aphasia caused by acute cerebral infarct. Prog Rehabil Med, 2016, 1: 20160008. [Medline]
29) Schulz R, Park E, Lee J, et al.: Synergistic but independent: the role of corticospinal and alternate motor fibers for residual motor output after stroke. Neuroimage Clin, 2017, 15: 118–124. [Medline] [CrossRef]
30) Lewis AF, Stewart JC: Comparison of corticospinal tract integrity measures extracted from standard versus native space in chronic stroke. J Neurosci Methods, 2021, 359: 109216. [Medline] [CrossRef]
31) Hernandez-Fernandez M, Reguly I, Jbabdi S, et al.: Using GPUs to accelerate computational diffusion MRI: from microstructure estimation to tractography and connectomes. Neuroimage, 2019, 188: 598–615. [Medline] [CrossRef]
32) Kim DH, Williams LJ, Hernandez-Fernandez M, et al.: Comparison of CPU and GPU bayesian estimates of fibre orientations from diffusion MRI. PLoS One, 2022, 17: e0252736. [Medline] [CrossRef]
33) Makris N, Kennedy DN, McInerney S, et al.: Segmentation of subcomponents within the superior longitudinal fascicle in humans: a quantitative, in vivo, DT-MRI study. Cereb Cortex, 2005, 15: 854–869. [Medline] [CrossRef]
34) Ivanova MV, Isaev DY, Dragoy OV, et al.: Diffusion-tensor imaging of major white matter tracts and their role in language processing in aphasia. Cortex, 2016, 85: 165–181. [Medline] [CrossRef]
35) Wang Y, Fernández-Miranda JC, Verstynen T, et al.: Rethinking the role of the middle longitudinal fascicle in language and auditory pathways. Cereb Cortex, 2013, 23: 2347–2356. [Medline] [CrossRef]
36) Mandonnet E, Nouet A, Gatignol P, et al.: Does the left inferior longitudinal fasciculus play a role in language? A brain stimulation study. Brain, 2007, 130: 623–629. [Medline] [CrossRef]
37) Koyama T, Marumoto K, Uchiyama Y, et al.: Outcome assessment of hemiparesis due to intracerebral hemorrhage using diffusion tensor fractional anisotropy. J Stroke Cerebrovasc Dis, 2015, 24: 881–889. [Medline] [CrossRef]